Optical Properties and Valence Change of Europium Ions in a Sol−Gel $Al_2O_3-B_2O_3-SiO_2$ Glass by Femtosecond Laser Pulses

Hongpeng You and Masayuki Nogami*

Department of Materials Science and Engineering, Nagoya Institute of Technology, Showa Nagoya, 466-8555, Japan

Received: March 27, 2005; In Final Form: June 7, 2005

The $Al_2O_3-B_2O_3-SiO_2$ glass containing europium ions was prepared by a sol−gel method. Fluorescence line-narrowing spectra (FLN) indicate two different environments of the Eu^{3+} ions. The calculated second crystal-field parameters exhibit the opposite behaviors of the two different environments. The FLN excitation and emission spectra before and after irradiation show that the change of the emission mainly comes from the Eu^{3+} ions at site I, revealing that the concentration ratio of the Eu^{3+} ions at site I to site II was decreased. The emission spectra confirmed that some Eu^{3+} ions were reduced into Eu^{2+} ions. The excitation spectra indicate that the Eu^{3+} ions at the sites with higher covalence degree can be easily reduced, implying that the Eu^{3+} ions are more easily reduced at site I than at site II. The absorption spectra before and after irradiation exhibit that the absorption of Eu^{2+} ions increases and that the positive hole centers appear. These results suggest a mechanism of the formation of the Eu^{2+} ions by femtosecond laser irradiation.

1. Introduction

Recent considerable research efforts have been made to manipulate three-dimensional (3D) microfabrication in materials using tightly focused femtosecond pulses[1−5] because femtosecond pulses provide a promising technique to fabricate optical device for potential applications such as optical waveguides,[1] waveguide amplifiers,[2] and 3D optical memory.[3] Among these applications, 3D optical memory has become of special importance because of its application in high-density optical data storage.[3,5] One potential method of the fabricating 3D optical memory is the valence manipulation of samarium ions in micrometer-scale dimension inside a transparent glass with femtosecond laser irradiation pulses, where the data information can be read out in the form of luminescence.[6] Therefore, some research works have been focused on the valence change of samarium ions via femtosecond laser irradiation.[6,7] On the other hand, several rare earth ions such as Eu^{3+}, Sm^{3+}, Yb^{3+}, and Tm^{3+} ions can be reduced at certain conditions.[8,9] Among these rare earth ions, the europium ion can be more easily reduced than the other rare earth ions. Moreover, europium ion plays an important role in the glass and crystal materials, which can act as a probe for structural evaluation[10−14] and as an activator for highly efficient red and blue phosphors.[15−17] These properties make it more available for the 3D optical memory. However, little attention was paid to it although the reduction from Eu^{3+} to Eu^{2+} ions was observed in the solution by femtosecond laser pulses that led to a little different change of the luminescent properties before and after irradiation.[18] This situation makes it difficult to store data information through the changes of luminescent properties. It is thus required to obtain the glass containing Eu^{3+} ions that can be easily reduced by femtosecond laser irradiation that can give rise to a large change of luminescent properties. In this paper, the $Al_2O_3-B_2O_3-SiO_2$ glass containing europium ions was prepared through a sol−gel process. The optical properties and valence change of europium ions in the glass before and after femtosecond laser irradiation were investigated. It was observed for the first time that the Eu^{3+} ions at sites with higher covalence degree can be more easily reduced than those at sites with lower covalence degree via femtosecond laser pulses. The luminescent properties of the europium ions in the glass exhibit a large difference before and after femtosecond laser irradiation, which may lead to potential application in the fabrication of 3D optical memory.

* Author to whom correspondence should be addressed. E-mail: nogami@mse.nitech.ac.jp.

2. Experimental Section

2.1. Sample Preparation. The $10Al_2O_3-5B_2O_3-85SiO_2-0.6Eu_2O_3$ glass was prepared by the sol−gel process using tetraethoxysilane (TEOS), $Al(OC_4H_9^{sec})_3$, $(B(OC_4H_9)_3$, $EuCl_3\cdot 6H_2O$, ethanol, and deionized water as the starting materials. A small amount of concentrated hydrochloric acid was added as a catalyst. The $Si(OC_2H_5)_4$ was first hydrolyzed with a mixed solution of ethanol and deionized water. $Al(OC_4H_9^{sec})_3$ and $(B(OC_4H_9)_3$ were then introduced into the partially hydrolyzed TEOS solution, followed by stirring for 1 h at about 70 °C. When the solution was cooled to room temperature, $EuCl_3\cdot 6H_2O$ dissolved in C_2H_5OH was added to this solution under stirring. The deionized H_2O (including 0.15mol/L HCl) was added and the resultant solution was stirred continuously for 30 min to form a homogeneous solution. The final solution was kept in plastic containers and was allowed to gel at room temperature for 4 weeks. The gel was heated at 900 °C in air for 4 h. The obtained glass was transparent and colorless. X-ray diffraction pattern shows that the glass is amorphous.

2.2. Characterization. The femtosecond pulse laser irradiation of the glass was performed by a Ti:sapphire regenerative amplifier laser system (Spectra Physics, Hurricane) operating at a wavelength of 800 nm with a 1 kHz repetition rate and

10.1021/jp051559u CCC: $30.25
Published on Web 07/06/2005

130 fs pulse duration. The laser beam with an average power of 600 mW was tightly focused on the sample through an objective lens. The spot size (diameter) of the laser beam was estimated to be 0.5 mm. To measure the optical properties of the glass after femtosecond laser irradiation, we irradiated a plane of 5.0×5.0 mm^2 in the glass by scanning the laser beam at a rate 1 mm/s.

The $^7F_0 \rightarrow {}^5D_0$ excitation and fluorescence line-narrowing (FLN) spectra were performed using the Jobin Yvon HR 320 monochromator at 8 K. A tunable dye laser (Rhodamine 6G: 566−640 nm) pumped by an Ar^+ laser (Coherent, Innova 70) was used as the excitation source. The laser line width was ~1.0 cm^{-1}. A chopper alternately opened the optical paths before and after the sample. The chopping frequency was 150 Hz. The $^7F_0 \rightarrow {}^5D_0$ excitation spectra were measured with scanning the output of the dye laser and monitoring the $^5D_0 \rightarrow {}^7F_2$ emission. The FLN spectra were obtained by exciting the $^7F_0 \rightarrow {}^5D_0$ transition.

The excitation and emission spectra were recorded at room temperature using a monochromator (Jobin Yvon, HR 320) and a photomultiplier (Hamamatsu, R955). A 500-W xenon lamp with light that passed through a monochromator (Jobin Yvon, H 20) was used as the excitation source. The fluorescence (FL) spectra were recorded using a N_2 laser with a 337-nm wavelength for excitation. A monochromator (Jobin Yvon, HR 320) combined with an image-intensified charge-coupled device (ICCD) camera was used for recording.

The optical absorption spectra were measured with an ultraviolet−visible spectrophotometer (JASCO, Ubest V-570, Tokyo, Japan).

3. Results and Discussion

3.1. FLN Spectra of the Eu^{3+} Ions in the Glass before and after Irradiation. The site of a Eu^{3+} ion in a glass is not sufficiently well defined to enable a simple characterization of its optical properties because glass does not have the ordered structure found in crystals. The emission band from Eu^{3+} ions, therefore, consists of a superposition of contributions from individual ions distributed among the entire ensemble of local environments. The resulting statistical distribution of Stark components leads to a significant degree of inhomogeneous broadening of the emission lines. The technique of laser-induced fluorescence line narrowing provides a microscopic probe of the local environment around the Eu^{3+} ion.[10−14] Crystal field analyses of FLN spectra can provide insight into the local structure, while analysis of the variation in the spectra as a function of excitation wavelength can obtain the information on the distribution of sites in the glass. Therefore, FLN spectra before and after femtosecond laser irradiation were measured and are shown in Figure 1. It can be seen that three groups of FLN lines at 17430−17190, 17180−16490, and 16500−15720 cm^{-1} are assigned to the $^5D_0 \rightarrow {}^7F_0$, $^5D_0 \rightarrow {}^7F_1$, and $^5D_0 \rightarrow {}^7F_2$ transitions, respectively. There are more than three lines of the $^5D_0 \rightarrow {}^7F_1$ transition, revealing at least two different environments for the Eu^{3+} ions in the glass. On the basis of the spectral features of the different excitation energies before irradiation, the $^5D_0 \rightarrow {}^7F_1$ transition bands can be separated into two groups (Figure 2), indicating that there are two kinds of environments (sites I and II) for the Eu^{3+} ions in the glass. Site I shows that the highest energy line significantly shifts to a higher energy side as the excitation energy increases, while the other two lines do not shift very much. This behavior of the Eu^{3+} ions at site I is quite similar to those of the Eu^{3+} ions doped oxide glasses, where the site symmetry of the Eu^{3+} ions is considered to be

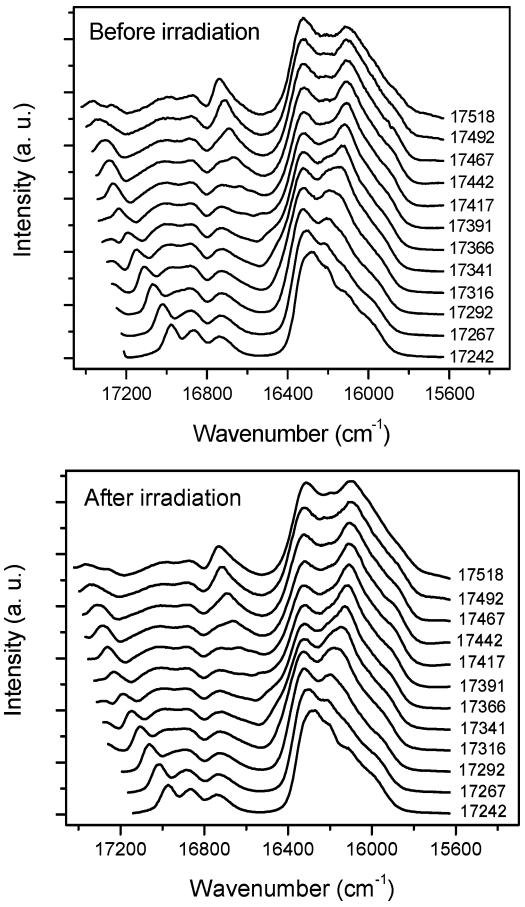

Figure 1. FLN spectra of the Eu^{3+} ions in the glass before and after irradiation, measured at 8 K. The numbers indicate the excitation wavenumber.

C_{2V}, C_2, or C_S.[12,14] The site symmetry of the Eu^{3+} ions at site I is thus restricted to C_{2V}, C_2, or C_S. On the other hand, site II exhibits a unique behavior; the lowest energy line shifts markedly to a lower energy side with increasing excitation energy, while the other two lines do not shift very much. Considering the splitting of the $^7F_1$ manifold into three levels, the site symmetry of the Eu^{3+} ion may be C_{2V}, C_2, C_1, or C_S. In C_{2V}, C_2, and C_S symmetries, the electron distribution of the $M_{J=0}$ component ($E(\epsilon_0)$) of the $^7F_1$ Stark levels differs from those of the other components ($E(\epsilon_-)$ and $E(\epsilon_+)$) of the $^7F_1$ Stark levels. In C_1 symmetry, there is not much difference in the symmetries of the three-wave functions. Therefore, it is suggested that the site symmetry of the Eu^{3+} ions at site II is also restricted to C_{2V}, C_2, or C_S.

To further investigate the change in the local structure of the Eu^{3+} ions in the glass, the second-order crystal parameters of the Eu^{3+} ions at sites I and II should be considered. The $M_{J=0}$ component ($E(\epsilon_0)$) is nondegenerate in all axial symmetries and does not mix with the others until all symmetries are removed. This fact should be reflected by the luminescent behavior of the $^5D_0 - {}^7F_1$ transitions. In the case of the Eu^{3+} ions at site I, the highest energy emission line of the three shifts much more than any other and is determined to be the $M_{J=0}$ component ($E(\epsilon_0)$). Unlike the case of the Eu^{3+} ions at site I, the Eu^{3+} ions at site II exhibit an opposite luminescent behavior. The lowest energy emission line should thus be assigned to the $M_{J=0}$ component ($E(\epsilon_0)$). The other two emission lines of sites I and II therefore belong to the $E(\epsilon_-)$ and $E(\epsilon_+)$ components although the ordering remains ambiguous. The energies of lines at sites I and II were used to estimate the

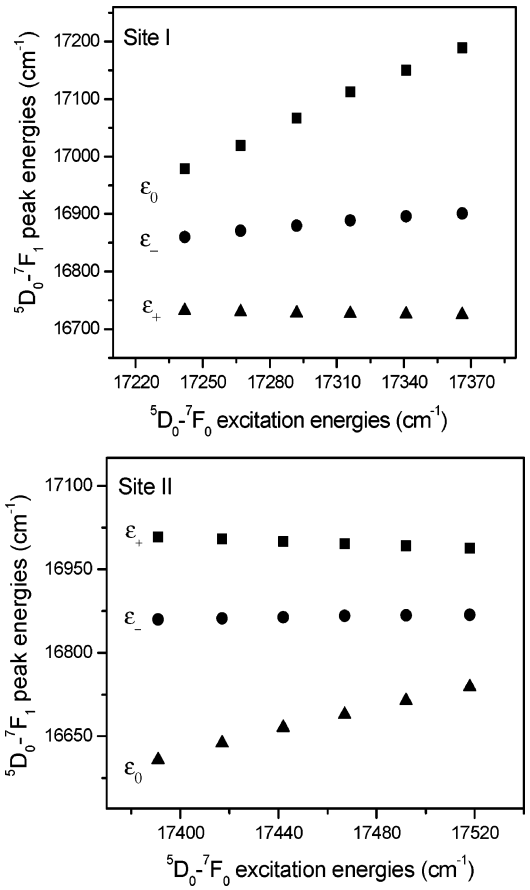

Figure 2. Peak energies of the three $^5D_0 \rightarrow {}^7F_1$ fluorescence lines of the Eu^{3+} ions in the glass at 8 K as a function of the $^7F_0 \rightarrow {}^5D_0$ excitation energy.

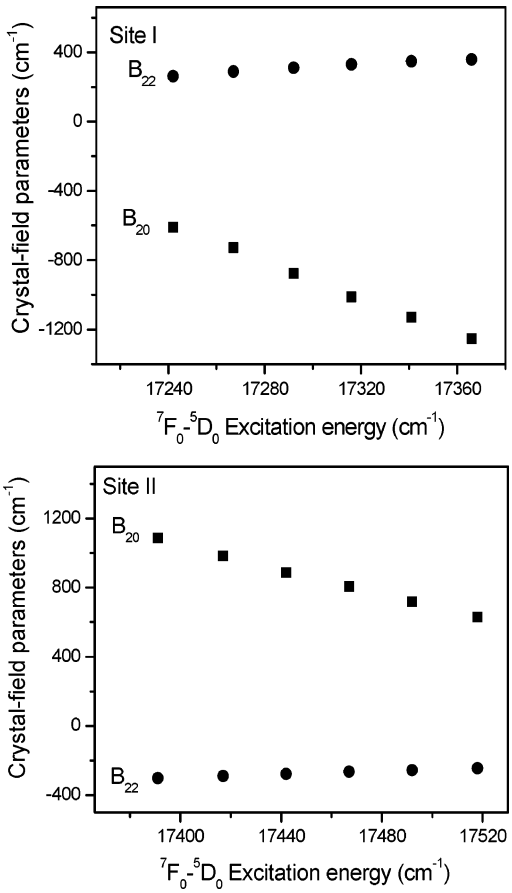

Figure 3. Second-order crystal-field parameters, B_{20} and B_{22}, of the Eu^{3+} ions in the glass as a function of $^7F_0 \rightarrow {}^5D_0$ excitation energy.

second-order crystal parameters on the basis of the following formulas:[12]

$$E(\epsilon_0) = E_0(^7F_1) + \frac{B_{20}}{5} \quad (1)$$

$$E(\epsilon_+) = E_0(^7F_1) - \frac{B_{20}}{10} + \frac{\sqrt{6}B_{22}}{10} \quad (2)$$

$$E(\epsilon_-) = E_0(^7F_1) - \frac{B_{20}}{10} - \frac{\sqrt{6}B_{22}}{10} \quad (3)$$

where $E_0(^7F_1)$ is the center of gravity of the $^7F_1$ multiplet, and $E(\epsilon_+)$, $E(\epsilon_-)$, and $E(\epsilon_0)$ are the energies of the corresponding components. The calculated second-order crystal field parameters, B_{20} and B_{22}, as a function of the excitation energy of the $^5D_0 \rightarrow {}^7F_0$ transition are shown in Figure 3. It can be seen that the sites I and II show different behaviors. The increase in the absolute values of both B_{20} and B_{22} at site I with the excitation energy indicates that the coordinating oxygen ions are closer to the Eu^{3+} ions at higher excitation energies.[11] In other words, there is a stronger crystal field in the Eu^{3+} ion surroundings. As a result, the $^7F_1$ level has a larger splitting. This result is in good agreement with our experimental observation. The decrease of absolute values of both B_{20} and B_{22} at site II with excitation energy reveals that the coordinating oxygen ions are farther away from the Eu^{3+} ions at higher excitation energies. This leads to the opposite behavior of the fluorescence lines of the Eu^{3+} ions at site II. The analysis of the FLN spectra mentioned above also indicates that the emission of the Eu^{3+} ions at site I mainly comes from lower energy excitation side, while the emission of the Eu^{3+} ions at site II mainly comes from higher energy excitation side.

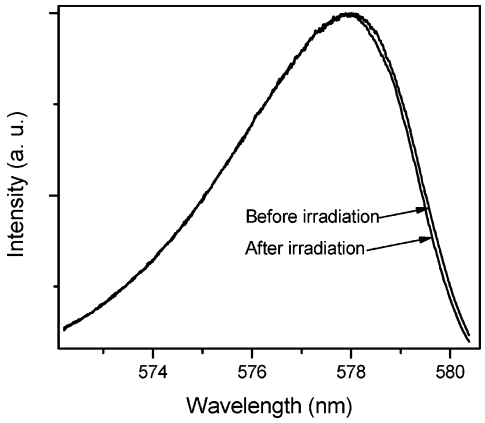

Figure 4. Excitation spectra of the $^5D_0 - {}^7F_0$ transition in the glass before and after femtosecond laser irradiation.

Compared the FLN spectra before and after irradiation, one can find that the intensity ratio of the peaks at about 16320 cm^{-1} to 16100 cm^{-1} is decreased although the excitation wavenumbers are the same for the emission spectra before and after irradiation. This fact suggests that the concentration ratio of the Eu^{3+} ions at different sites was changed after femtosecond laser irradiation. To further elucidate the detailed change of the Eu^{3+} ions at sites I and II, the FLN excitation spectra before and after femtosecond laser irradiation were measured and are given in Figure 4. It shows that the change of the emission mainly comes from the lower excitation energy side. This

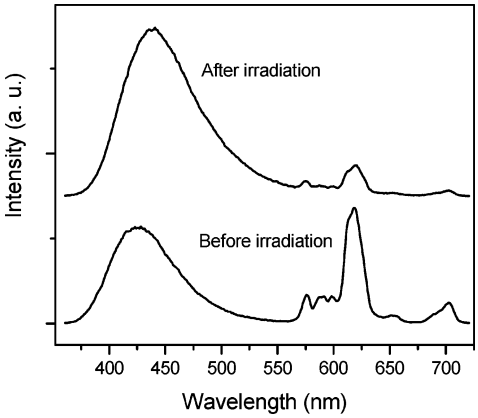

Figure 5. Emission spectra of the glass before and after femtosecond laser irradiation ($\lambda_{ex} = 337$ nm).

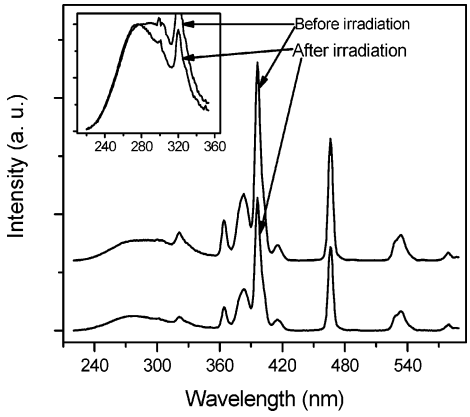

Figure 6. Excitation spectra of the Eu^{3+} ions in the glass before and after femtosecond laser irradiation ($\lambda_{em} = 618$ nm).

observation means that the concentration of the Eu^{3+} ions at site I, compared with that of the Eu^{3+} ions at site II, was decreased. In general, femtosecond laser pulses can easily lead to the reduction of samarium from Sm^{3+} to Sm^{2+} ions in glasses. Furthermore, femtosecond laser pulses can give rise to the valence change of europium ions in solution.[18] We therefore inferred that some Eu^{3+} ions were reduced into Eu^{2+} ions during femtosecond laser irradiation. Our inference was confirmed by the change of the emission spectra before and after irradiation.

3.2. Emission and Excitation Spectra of the Europium Ions in the Glass before and after Irradiation. The emission spectra before and after irradiation are given in Figure 5. It can be seen that the emission spectrum of the glass before irradiation consists of a broad band and several narrow bands. The broad band at about 425 nm is due to the allowed 5d−4f transition of the Eu^{2+} ions. The narrow bands at about 576, 589, 598, 618, 653, and 702 nm are attributed to the $^5D_0-^7F_J$ ($J = 0, 1, 1, 2, 3, 4$) transitions of the Eu^{3+} ions, respectively.

After irradiation, the emission intensity of the 5d−4f transitions of Eu^{2+} ions increases. Moreover, the emission band of the 5d−4f transitions of Eu^{2+} ions shifts to lower energy side. On the other hand, the emission intensity of Eu^{3+} ions drastically decreases. These phenomena are associated with the concentration change between Eu^{2+} and Eu^{3+} ions. The increase of emission intensity of the Eu^{2+} ions implies that the concentration of Eu^{2+} ions increases, while the decrease of emission intensity of the Eu^{3+} ions indicates that the concentration of Eu^{3+} ions decreases. This experimental result confirms that some Eu^{3+} ions were reduced into Eu^{2+} ions under femtosecond laser irradiation.

Figure 6 gives the excitation spectra of Eu^{3+} ions in $10Al_2O_3-5B_2O_3-85SiO_2$ glass before and after femtosecond laser irradiation. The excitation spectrum of the glass before irradiation consists of a broad band and several narrow bands. The broad band in the range from 220 to 340 nm is due to the charge-transfer absorption of the Eu^{3+} ion. The narrow bands at about 320, 364, 383, 395, 416, 466, 532, and 577 nm are attributed to the f−f transition absorptions within the Eu^{3+} $4f^6$ configuration. The intensities of the excitation bands are decreased after irradiation. It indicates that some Eu^{3+} ions were reduced into Eu^{2+} ions via femtosecond laser irradiation. It is significant to note that the intensity decrease of the charge-transfer band at the lower energy side is larger than that of the charge-transfer band at the higher energy side. This demonstrates that the Eu^{3+} ions that occupied the sites with lower charge-transfer energy can be easily reduced; that is to say, the Eu^{3+} ions at sites with higher covalence degree can be easily reduced.

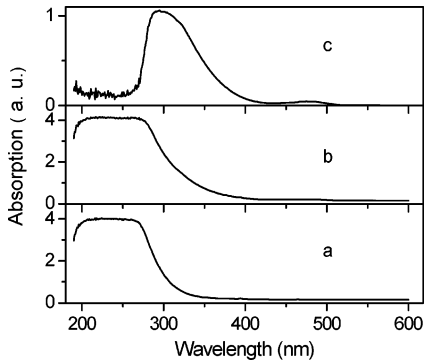

Figure 7. Absorption spectra of the glass before (a) and after (b) femtosecond laser irradiation, difference absorption spectrum (c).

This result is also in agreement with the observation of the FLN excitation spectra of the $^5D_0-^7F_0$ transition (Figure 4). Since the charge-transfer band of the Eu^{3+} ions is created by the electron transition from the surrounding oxygen ion to the Eu^{3+} ion, the stronger ability to attract the electron from the oxygen ion and the higher covalence degree, the lower energy is required for transferring the electron from the surrounding oxygen ion to the Eu^{3+} ion. This implies that the Eu^{3+} ion at the sites with lower charge-transfer energy are more easily reduced than those at the sites with higher charge-transfer energy. This theoretical explanation supports our experimental observation. Considering the result of the FLN spectra and the change of excitation spectra before and after irradiation, the Eu^{3+} ions at site I can be more easily reduced than those at site II.

3.3. Absorption Spectra before and after Irradiation. Figure 7 gives the absorption spectra before and after the femtosecond laser irradiation. The broad bands in the range from 200 to 350 nm are assigned to the charge-transfer absorption of the Eu^{3+} ions and the 4f−5d transition absorption of the Eu^{2+} ions. The absorption band after the irradiation was broadened. The difference absorption spectrum is presented in Figure 7c. It discloses that the laser irradiation causes the absorption band change in the range from 200 to 500 nm. The increased absorption in the range from 200 to 410 nm is mainly due to the absorption of the 4f−5d transition of the Eu^{2+} ions that was created by the femtosecond laser irradiation. The increased absorption in the range from 400 to 500 nm is quite similar to the optical absorption in the similar range induced by the gamma irradiation in some borate and silicate glasses. The nature of the induced optical absorption in the similar range is assigned to the absorption of positive hole centers.[19] It is therefore reasonable that the increased absorption in the range from 400 to 500 nm is due to the absorption of the positive hole centers.

3.4. Mechanism of the Formation of the Eu^{2+} Ions by Femtosecond Laser Irradiation. It is well-known that femtosecond laser pulses can create electrons and holes in the materials throughout multiphoton excitation.[20−22] Thus, the experimental results mentioned above suggest a mechanism to describe the processes that can lead to the formation of the Eu^{2+} ions in the glass under the femtosecond laser irradiation. The mechanism involves the band structure and defects in the glass. The irradiation of the glass by femtosecond laser creates electron−hole pairs by band-to-band transition via multiphoton excitation. This means that the electrons are delocalized from the valence band (VB) and transferred to the conduction band (CB). The electrons and holes are redistributed throughout the conduction and valence bands. As a result, some electrons were trapped by the Eu^{3+} ions which led to the formation of the Eu^{2+} ions. Some holes were trapped by the trapped centers that gave rise to the appearance of the positive hole centers which induced unique absorption in the range from 400 to 500 nm.

4. Conclusion

In this study, the optical properties and valance change of the Eu^{3+} ions in the $Al_2O_3-B_2O_3-SiO_2$ glass were investigated. The analysis of the FLN spectra indicates that there are two kinds of surroundings of the Eu^{3+} ions. The second-order crystal field analysis of the $^7F_1$ Stark splitting reveals that the coordinating oxygen ions of site I are closer to the Eu^{3+} ions and those of site II are father away from the Eu^{3+} ions with increased excitation energy. As a result, the fluorescent lines of the Eu^{3+} ions at sites I and II exhibit different behaviors. The emission spectra confirm that some Eu^{3+} ions can be reduced into Eu^{2+} ions under femtosecond laser irradiation. The excitation spectra reveal that the Eu^{3+} ions at sites with higher covalence degree can be more easily reduced than those at sites with lower covalence degree. This finding provides the theoretical fundaments for predicting, designing, and synthesizing new glasses containing Eu^{3+} ions which can be more easily reduced by femtosecond laser irradiation. The increased absorption in the range from 400 to 500 nm originates from the absorption of the positive hole centers. It is suggested that the electrons and holes are redistributed throughout the conduction and valence bands via multiphoton excitation that lead to the formation of the Eu^{2+} ions in the glass.

Acknowledgment. This research was partly supported by the NITECH 21st Century COE Program for Environment-Friendly Ceramics.

References and Notes

(1) Miura, K.; Qiu, J.; Inouye, H.; Mitsuyu, T.; Hirao, K. *Appl. Phys. Lett.* **1997**, *71*, 3329−3331.
(2) Sikorski, Y.; Said, A. A.; Bado, P.; Maynard, R.; Florea, C.; Winick, K. A. *Electron. Lett.* **2000**, *36*, 226−227.
(3) Watanabe, M.; Juodkazis, S.; Sun, H. B.; Matsuo, S.; Misawa, H. *Appl. Phys. Lett.* **2000**, *77*, 13−15.
(4) Zhou, W.; Kuebler, S. M.; Braun, K. L.; Yu, T.; Cammack J. K.; Ober, C. K.; Perry, J. W.; Marder, S. R. *Science* **2002**, *296*, 1106−1109.
(5) Gourevich, I.; Pham, H.; Jonkman, J. E. N.; Kumacheva, E. *Chem. Mater.* **2004**, *16*, 1472−1479.
(6) Qiu, J.; Miura, K.; Suzuki, T.; Mitsuyu, T. *Appl. Phys. Lett.* **1999**,*74*, 10−12.
(7) Park, G. J.; Hayakawa, T.; Nogami, M. *J. Phys.: Condens. Matter* **2003**, *15* 1259−1265.
(8) Peterson, J. R.; Xu, W.; Dail, S. *Chem. Mater.* **1995**, *7*, 1686−1689.
(9) Peng, M.; Pei, Z.; Hong, G.; Su, Q. *Chem. Phys. Lett*. **2003**, *371*, 1−6.
(10) Berecher, C.; Riseberg, L. A. *Phys. Rev. B* **1976**, *13*, 81−93.
(11) Belliveau, T. F.; Simkin, D. J. *J. Non-Cryst. Solids* **1989**, *110*, 127−141.
(12) Tanaka, M.; Nishimura, G.; Kushida, T. *Phys. Rev. B* **1994**, *49*, 16917−6925.
(13) Stone, B. T.; Costa, V. C.; Bray, K. L. *Chem. Mater*. **1997**, *9*, 2592−2598, and references therein.
(14) You, H.; Nogami, M. *J. Phys. Chem. B* **2004**, *108*, 12003−12008.
(15) Frindell, K. L.; Bartl, M. H.; Popitsch, A.; Stucky, G. D. *Angew Chem., Int. Ed.* **2002**, *41*, 959−962.
(16) Feldmann, C.; Jüstel, T.; Ronda, C. R.; Schmidt, P. J. *Adv. Funct. Mater.* **2003**, *13*, 511−516.
(17) Xie, R.; Hirosaki, N.; Mitomo, M.; Yamamoto, Y.; Suehiro, T.; Sakuma, K. *J. Phys. Chem. B* **2004**, *108*, 12027−12031.
(18) Nakashima, N.; Nakamura, S.; Sakabe, S.; Schillinger, H.; Hamanaka, Y.; Yamanaka, C.; Kusaba, M.; Ishihara, N.; Izawa, Y. *J. Phys. Chem. A* **1999**, 103, 3910−3916.
(19) Bishay, D. *J. Non-Cryst. Solids* **1970**, *3*, 54−114, and references therein.
(20) Stuart, B. C.; Feit, M. D.; Rubenchik, A. M.; Shore, B. W.; Perry, M. D. *Phys. Rev. Lett*. **1995**, *74*, 2248−2251.
(21) Sun, H.; Juodkazis, S.; Watanabe, M.; Matsuo, S.; Misawa, H.; Nishii, J. *J. Phys. Chem. B* **2000**, *104*, 3450−3455.
(22) Sundaram S. K.; Mazur, E. *Nat. Mater*. **2002**, *1*, 217−224.